AADE-06-DF-HO-03

Annular Flow-Loop Studies of Non-Newtonian Reservoir Drilling Fluids
Sanjit Roy and Mario Zamora, M-I SWACO

Abstract

This paper presents results from a series of annular flow-loop experiments conducted on biopolymer and heavy brine reservoir drilling fluids. Experiments were designed to measure frictional pressure losses and document flow instabilities for different combinations of drill-pipe eccentricity and rotation, flow rate, and flow regime. The purpose of these studies was to generate new data to improve the understanding of flow behavior of non-Newtonian fluids in annular geometries and to enhance hydraulics models for calculating annular pressure losses.

Testing was conducted using a laboratory scale-up flow loop designed for rotary speeds up to 950 rpm. The transparent outer tube permitted inspection and video documentation of rotation-induced instabilities.

Introduction

Owing to their importance to the drilling operation, the effects of drill-pipe rotation on axial flow of non-Newtonian fluids in annular geometries have received considerable attention in theoretical analyses, laboratory evaluations, and well measurements. This has also been a topic of debate due to apparent conflicting results among different studies, the lack of quality laboratory and field data, and the difficulties with development of analytical models.

Wellsite pressure measurements invariably indicate that drill-pipe rotation increases annular pressure losses.[1,2,3] However, field data analyses are complicated by variable downhole properties and the number, complexity, and interdependency of key parameters.[4,5] It is generally thought that some of the pressure increases are caused by cuttings bed resuspension, but similar behavior has been reported in cased holes without cuttings.[6,7,8] The rate of change of rotation also is important since rapid increases in thixotropic fluids can cause downhole pressure losses to be initially higher than steady state values.[1]

The impact of rotation can be classified based on three zones that depend on a rotational to axial velocity ratio.[9] If axial flow dominates (ratio < 1), shear thinning creates a low-viscosity layer around the drill pipe and reduces pressure loss. If rotational velocity dominates (ratio > 10), a low-velocity, high-viscosity recirculation region appears in the cross-flow plane that can increase pressure loss. The recirculation regions disappear at very high Taylor numbers (>50,000) or when fluid n-factor values are low (<0.2). For intermediate ratios, flow behavior is mixed and pressure losses generally increase with increasing velocity ratio.

The Taylor number is a dimensionless quantity used to characterize instabilities in rotating annular geometries. Analogous to the Reynolds number used in axial flow, flow in a narrow-gap annulus is considered unstable if the Taylor number is greater than a critical value.

The primary purpose of this paper is to present results from experimental investigations into rotation effects on annular pressure over a range of fluid properties, flow regimes, eccentricities, and rotary speeds. Most of the fluids tested in this flow loop over time have been water based; results presented in this paper are based on six of those fluids. Also discussed are visual observations of complex flow patterns caused by rotation-induced instabilities at low axial flow rates.

Experimental Setup and Test Procedure

Experiments were conducted in a vertically mounted, narrow-gap annular test section that was original constructed to investigate slimhole hydraulics.[10] The test section consisted of a 5.5-ft by 1.75-in. ID cast acrylic tube with a 1.25-in. stainless steel inner shaft that could be rotated to 950 rpm with minimal vibration. The outer tube could be repositioned to vary the eccentricity from concentric to fully eccentric. A variable-speed, positive-displacement pump delivered flow rates to 20 gal/min at pressures up to 30 psi. A flow bypass system was implemented to ensure stable flow rates below approximately 5 gal/min.

Primary test metrics included differential pressure, flow rate, fluid density, shaft rotational speed, and fluid temperature. A Coriolis mass flow meter measured flow rate, density and temperature. Differential pressure gages measured pressure loss across a 4-ft span of the test section, while an optical encoder measured shaft rotational speed.

The flow loop was designed with a transparent outer tube to permit study and documentation of rotation-induced instabilities in the form of Taylor vortices. A

high-resolution video camera recorded vortices formation and behavior with low axial velocity and full range of drill-pipe rotary speeds. A separate camera simultaneously captured engineering data from the data acquisition system. Different materials, including air bubbles and small plastic beads, were introduced into the flow system to highlight the Taylor vortices during tests with concentric drill pipe.

Hydraulics tests consisted of measuring differential pressure in the test section for different flow rates, drill-pipe eccentricity, and rotational speeds. Two different sets of experiments were conducted. The first was designed to determine the effects of eccentricity without rotation. The second targeted the effects of rotation with different eccentricities at constant flow rates. Flow rates ranged from 1 to 19 gal/min, eccentricities from 0 (concentric) to 100% (fully eccentric), and rotation speeds from 0 to 950 rpm. In contrast, previous studies such as those cited in this paper were typically limited to narrower ranges of conditions.

Variable flow rate experiments were started at the highest flow rate, but data were collected while ramping both down and up. Rotation tests started with no rotation, and both ramping up and down data were collected. Transient effects due to changing flow rate or rotation were minimized by allowing time for test conditions to stabilize. Flow-loop temperatures were not controlled; however, temperature variations were less than 2°F due to the relatively low system pressure losses.

Experimental data were collected for different Newtonian and non-Newtonian water-based fluids, some of which represented typical reservoir drilling fluids. The list of lab-prepared and field-supplied test fluids in **Table 1** includes key rheological properties. The wide range of fluid viscosities made it possible to run tests in laminar, transitional, and turbulent flow. Fresh water also was tested to verify equipment and test consistency.

Experimental Results

For clarity, results are grouped into sections showing the effects of eccentricity on pressure loss with no rotation, and the effects of rotation on pressure loss with and without rotation. Rotation test results are further grouped based on flow regime in axial flow. For rotation tests, pressure loss data were normalized with respect to results without rotation. Flow visualization data are presented as images digitized from video recordings.

Effects of Eccentricity without Rotation

Fig. 1 shows Fluid A (fresh water) pressure losses without drill-pipe rotation as a function of flow rate and eccentricity. Note that the concave shapes of the curves in the rectilinear plot are consistent with turbulent flow. Only turbulent flow data could be collected because of the low viscosity of the fresh water. As expected and consistent with published results, annular pressure loss

decreased with increasing eccentricity.[11] Measured data also matched pressure losses calculated based on published models.[12] These tests also help verify that the equipment was operating properly.

Fig. 2 shows the effects of eccentricity on pressure loss for the Fluid D biopolymer field reservoir drilling fluid. The viscosity was such that only laminar flow could be achieved in the flow loop as demonstrated by the characteristic convex shape of the curves. Similar to the turbulent flow data, pressure losses decreased with increasing drill-pipe eccentricity and matched calculated pressure losses well.

Effects of Rotation with Turbulent Axial Flow

Fig. 3a presents rotation effects on pressure loss for Fluid A in the concentric annulus. Pressure loss increased with rotation at all flow rates as shown by the ratio of rotating and non-rotating pressures being greater than 1. **Figs. 3b** and **3c** shows the effects of rotation at 50% and 75% eccentricities, respectively. While trends were similar, the impact of rotation was greater with eccentric than concentric drill pipe. In all cases, rotation had a bigger effect at lower flow rates. Contrasting **Figs. 3b** and **3c**, the impact of rotation at 50% eccentricity was greater than that at 75% at lower flow rates. These results are consistent with published data.[13,14]

The effects of rotation on Fluid B (cesium formate) pressure losses tested with different eccentricities are presented in **Figs. 4a - 4c**. Similar to the freshwater results, the pressure losses always increased with rotation, and the impact was larger for intermediate eccentricity (50%) and for lower flow rates.

Effects of Rotation with Laminar Axial Flow

Only laminar axial flow could be obtained for the high-viscosity Fluid C (26-lb_m/bbl bentonite slurry) and Fluid D (biopolymer field mud) test samples. **Fig. 5a** shows that for Fluid C with concentric drill pipe, pressure loss always decreased with rotation. The impact of rotation was more significant at lower flow rates. Little effect was noted at higher flow rates indicating that high axial velocities dominated rotational effects.

In general, most previous lab studies indicated pressure loss decreases with rotation for different fluids in laminar flow.[9,10,13,15,16] Some studies, however, have demonstrated that rotation has no effect on pressure loss for Newtonian fluids with concentric drill pipe in laminar flow.[17] Others have shown that for non-Newtonian fluids, pressure loss initially decreases and then increases with rotation.[18] Field measurements have suggested that transverse drill-pipe vibrations induced by rotation could result in higher pressure losses even for laminar flow without rotation.[19]

At intermediate eccentricities (50%), pressure loss decreased with rotation at lower flow rates as shown in **Fig. 5b**, probably because shear-thinning effects suppressed inertial effects.[14] At higher flow rates (>9

gal/min), pressure loss increased with drill-pipe rotation, and the impact of rotation was larger as flow rate was increased. As shown in **Fig. 5c**, 75% eccentricity results were similar to the concentric case except at 19 gal/min, where pressure losses increased slightly with rotation.

Figs. 6a-6c illustrate the effects of rotation on pressure loss with Fluid D and different drill-pipe eccentricities. When concentric, pressure losses decreased with rotation at lower flow rates and rotary speeds. Pressure losses increased at higher flow rates and rotary speeds. When the pressure loss ratio was less than 1, rotation had a lesser impact at higher flow rates. For ratios greater than 1, rotation had a larger impact at higher flow rates. Trends were similar with eccentricity; however, there was a change in the transition flow rate when the pressure loss ratio was greater than 1. At the intermediate eccentricity, the transition was at approximately 3.5 gal/min; for 75% eccentricity, it was greater than 5 gal/min.

Considerable debate continues on the coupled effects of rotation and eccentricity. Numerical studies indicate that for non-Newtonian fluids, inertial effects counteract fluid shear-thinning characteristics.[14] With slightly eccentric pipe, shear-thinning effects dominate inertial effects, and pressure losses decrease with rotation. The effect is more pronounced as the fluid n-value decreases. With highly eccentric pipe, inertial effects dominate and pressure losses increase with rotation. At intermediate eccentricities, shear-thinning has a similar effect as the inertial effects at low rotation, and acts in a counteracting role at high rotary speeds. Hence, pressure losses could first increase, and then decrease with rotation speed for high n values. The critical Taylor number for the onset of vortices increases as eccentricity is increased.

Effects of Rotation with Laminar and Turbulent Axial Flow

Laminar, transitional, and turbulent flow was achievable with Fluid E (18-lb_m/bbl bentonite slurry) without rotation and for all drill-pipe eccentricities. **Fig. 7** shows the effects of eccentricity on pressure loss. As expected, pressure losses decreased with eccentricity in both laminar and turbulent axial flow. In transitional flow from 11-14 gal/min, however, eccentricity had little effect on pressure loss, similar to some published data.[20] Calculated data matched measured pressure losses in laminar and turbulent flow, but were lower in transitional flow.

At low flow rates, pressure losses decreased with rotation for Fluid E with concentric drill pipe as presented in **Fig. 8a**. Pressure loss increased with rotation at higher flow rates, even though axial flow was laminar without rotation, suggesting induced turbulence due to centrifugal instability.[21-24] Field measurements have shown that when the Taylor number was higher than the critical Taylor number, pressure losses increased with

rotation even though axial flow was laminar without rotation.[1,13]

Pressure loss increased for all flow rates with rotation at 50% and 75% eccentricities as shown in **Figs. 8b** and **8c**. Even at low flow rates where the axial flow was laminar without rotation, pressure losses increased with rotation suggesting that centrifugal instability may have induced turbulence. Rotation had the greatest impact at intermediate flow rates for all eccentricities.

Effect of Rotation with Drag Reduction

The small concentration of biopolymer in Fluid F resulted in drag reduction in turbulent flow. The friction-factor plot (**Fig. 9**) demonstrates the delayed onset of turbulence and the lower-than-expected measured pressure losses.

Figs. 10a - 10c show the effects of rotation on pressure loss for Fluid F with different drill-pipe eccentricities. With concentric drill pipe, results were similar to Fluid E as pressure losses decreased with rotation at low flow rates. However, pressure losses increased at intermediate flow rates even though flow was laminar without rotation. With eccentric pipe, pressure losses increased with rotation except at very low flow rates, and the impact of rotation was higher at intermediate flow rates. It appears that drag reduction did not influence rotation effects on pressure loss.

Flow Visualization

Annular fluid motion resembles Couette flow in a rotational viscometer with slow rotary speeds and no axial velocity. Addition of axial flow usually results in helical motion with both tangential and axial components. As rotary speed is increased, centrifugal forces can fling fluid away from drill pipe, thereby creating a void that is filled by fluid from the outer part of annulus. This causes secondary flows of ring-like patterns called Taylor vortices. Even though higher axial flows disrupt these ordered vortices, they have been shown to exist with significant axial flow.[25-27]

Flow visualization tests (**Figs. 11-14**) were performed with Fluid G that contained 2-lb_m/bbl HEC. A red dye was added to accentuate Taylor vortices. **Fig. 11** shows a screen capture with sensor data automatically superimposed over flow loop video. Video outputs from the two cameras were passed through a Digital AV Mixer to provide a real-time, simultaneous, split-screen view of both the test section and the data acquisition computer screen.[28] Taylor vortices were clearly visible in the test section at mass flow rate of 5 lb_m/min and 900 rpm.

Fig. 12 shows screen captures of Taylor vortices as rotary speed was systematically increased from 700 to 900 rpm, at a constant flow rate of 0.6 gal/min. As rotary speed increased, the Taylor vortices were better defined and separated from each other.

Between 750 and 900 rpm, behavior of the Taylor vortices changed from paired rings rotating about their

own axis in opposite directions to toroidal Taylor vortices that started translating with the axial flow. Successive screen captures in **Fig. 13** show downstream translation of individual vortices, opposite to the axial flow direction at rotary speed close to 900 rpm. Below 750 rpm, the vortices were essentially closed, stationary cells. The individual vortices moved opposite to the axial flow direction up to about 900 rpm, after which they stabilized and stopped translating axially.

Fig. 14 shows screen captures of Taylor vortices at various levels of flow rate with 900-rpm rotary speed. With increasing flow rate, the Taylor vortices pattern changed from toroidal to helical, and the only evidence of the vortices was the sinous nature of the flow. It has been experimentally shown that while not readily visible at higher flow rates, helical vortices exist even though the axial flow overwhelms the velocity related to the vortical motion.[27]

Conclusions

1. Experimental data suggest there are definite trends in the effects of rotation on annular pressure loss in laminar and turbulent flow with both concentric and eccentric pipe.
2. Pipe eccentricity reduced pressure losses in laminar and turbulent axial flow. There was little effect of eccentricity in transitional flow.
3. In the absence of rotation-induced instabilities, annular pressure losses increased in turbulent flow, and decreased in laminar flow with rotary speed.
4. Rotation-induced instabilities at high Taylor numbers, especially with eccentric geometries, resulted in pressure-loss increases with rotation even though axial Reynolds numbers without rotation were below the expected critical value.
5. With laminar flow, the impact of rotation (measured as ratio of rotating to non-rotating pressure loss) monotonously increased with higher flow rates. In full turbulent flow, the impact of rotation decreased with increasing flow rate. In all other cases, the impact of rotation was higher at intermediate flow rates.
6. Eccentricity combined with rotation had a complex effect on pressure loss. In laminar flow, higher eccentricities helped induce turbulent instabilities, resulting in higher rotating pressure losses. In turbulent flow, rotation had a bigger impact on pressure loss with eccentric pipe.
7. With increasing axial flow, rotation-induced instabilities occurred at lower rotary speeds.
8. Analytical models or empirical equations could not be developed from this new data to analytically address rotation effects on annular pressure loss with Herschel-Bulkley fluids with eccentric drill pipe.

References

1. Marken, C. D., He, X., and Saasen, A.: "The Influence of Drilling Conditions on Annular Pressure Losses," SPE 24598, SPE Annual Technical Conference, Washington DC, Oct 4-7, 1992.
2. Bode, D. J., Noffke, R. B., and Nickens, H. V.: "Well-Control Methods and Practices in Small-Diameter Wellbores," *Journal of Petroleum Technology* (Nov 1991) 1380.
3. Delwiche, R. A., Lejeune, M. W. D., Mawet, P. F. B. N., and Vighetto, R.: "Slimhole Drilling Hydraulics," SPE 24596, SPE Annual Technical Conference, Washington DC, Oct 4-7, 1992.
4. Minton, R. C., and Bern, P. A.: "Field Measurement and Analysis of Circulating System Pressure Drops with Low-Toxicity Oil Based Drilling Fluids," SPE 17242, SPE/IADC Drilling Conference, Dallas, Feb 28 – Mar 2, 1988.
5. Zamora, M.: "Virtual Rheology and Hydraulics Improve Use of Oil and Synthetic-Based Muds," *Oil & Gas Journal* (Mar 3, 1997) 43.
6. Aldred, W., Cook, J., Bern, P. A., Carpenter, W., Hutchinson, M., Lovell, J., Rezmer-Cooper, I., and Leder, P. C.: "Using Downhole Annular Pressure Measurements to Improve Drilling Performance," *Schlumberger Oilfield Review* (Winter 1998) 40.
7. Green, M. D., Thomesen, C. R., Wolfson, L., and Bern, P. A.: "An Integrated Solution of Extended-Reach Drilling Problems in the Niakuk Field, Alska: Part II- Hydraulics, Cuttings Transport and PWD," SPE 56564, SPE Annual Technical Conference, Houston, Oct 3-6, 1999.
8. Ward, C. and Andreassen, E.: "Pressure-While-Drilling Data Improve Reservoir Drilling Performance," *SPE Drilling and Completion,* v. 13, no. 1 (Mar 1998) 19.
9. Escudier, M.P., Oliviera, P. J., and Pinho, F. T.: "Fully Developed Laminar Flow of Purely Viscous non-Newtonian Fluids Through Annuli, Including the Effects of Eccentricity and Inner-cylinder Rotation," *International Journal of Heat and Fluid Flow,* v. 23 (2002) 52.
10. Haciislamoglu, M. and Cartalos, U.: "Practical Pressure Loss Predictions in Realistic Annular Geometries," SPE 28304, SPE Annual Technical Conference, New Orleans, Sept 25-28, 1994.
11. Zamora, M., Roy, S., and Slater, K.: "Comparing a Basic Set of Drilling Fluid Pressure-Loss Relationships to Flow-Loop and Field Data," AADE-05-NTCE-27, AADE National Technical Conference, Houston, April 5-7, 2005.
12. Hansen, S. A. and Sterri, N.: "Drill Pipe Rotation Effects on Frictional Pressure Losses in Slim Annuli," SPE 30488, SPE Annual Technical Conference, Dallas, Oct 22-25, 1995.
13. Wan, S., Morrison, D., and Bryden, I. G.: "The Flow of Newtonian and Inelastic non-Newtonian Fluids in Eccentric Annuli with Inner-Cylinder Rotation," *Theoretical and Computational Fluid Dynamics,* v. 13 (2000) 349.
14. Walker, R. E., and al-Rawi, O.: "Helical Flow of Bentonite

Slurries," SPE 3108, SPE Annual Fall Meeting, Houston, Oct 4-7, 1970.

15. Bird, R. B., Armstrong, R. C., and Hassager, O.: *Dynamics of Polymeric Liquids,* Vol. 1, 2nd ed.; Wiley (1987).

16. McCann, R. C., Quigley, M. S., Zamora, M. and Slater, K. S.: "Effects of High-Speed Pipe Rotation on Pressures in Narrow Annuli," *SPE Drilling and Completions* (June 1995) 96.

17. Ooms, G., and Kampman-Reinhartz, B. E.: "Influence of Drillpipe Rotation and Eccentricity on Pressure Drop over Borehole During Drilling," SPE 56638, SPE Annual Technical Conference, Houston, Oct 3-6, 1999.

18. Hemphill, T. and Ravi, K.: "Calculation of Drillpipe Rotation Effects on Fluids in Axial Flow: An Engineering Approach," SPE 97158, SPE Annual Technical Conference, Dallas, Oct 9-12, 2005.

19. Cartalos, U. and Dupuis, D.: "An Analysis Accounting for the Combined Effect of Drillstring Rotation and Eccentricity on Pressure Losses in Slimhole Drilling," SPE 25769, SPE/IADC Drilling Conference, Amsterdam, Feb 23-25, 1993.

20. Cartalos, U., King, I., Dupuis, D., and Sagot, A.: "Field Validated Hydraulic Model Predictions Give Guidelines for Optimal Annular Flow in Slimhole Drilling," SPE 35131, SPE/IADC Drilling Conference, New Orleans, Mar 12-15, 1996.

21. Chandrasekhar, S.: *Hydrodynamic and Hydromagnetic Stability*, Oxford (1961).

22. Simmers, D. A. and Coney, J. E. R.: "A Reynolds Analogy Solution for the Heat Transfer Characteristic of combined Taylor Vortex and Axial Flows," *International Journal of Heat and Mass Transfer, v. 22, no. 5* (1979) 679.

23. Drazin, P. G., and Reid, W. H.: *Hydrodynamic Stability*, Cambridge University Press, Cambridge (1981).

24. Barnes, H. A., Hutton, J. F., and Walters, K.: *An Introduction to Rheology*, Elsevier (1989).

25. Lockett, T.J., Richardson, S. M., and Worraker, W. J.: "The Importance of Rotation Effects for Efficient Cuttings Removal During Drilling," SPE 25768, SPE/IADC Drilling Conference, Amsterdam, Feb 23-25, 1993.

26. Kaye, J. and Elgar, E.C.: "Modes of Adiabatic and Diabatic Fluid Flow in an Annulus with an Inner Rotating Cylinder," *Trans. ASME* (April 1958) 753.

27. Wereley, S. T., and Lueptow, R. M.: "Velocity Field for Taylor-Couette Flow with an Axial Flow," *Physics of Fluids* v. 11, no. 12 (1999) 3637.

28. Zamora, M. and Jefferson, D. T.: "Flow Visualization of Solids Transport by Drilling Fluids in Inclined Wells," *Developments in Non-Newtonian Flows*, ASME, AMD-vol. 175 (1993) 115.

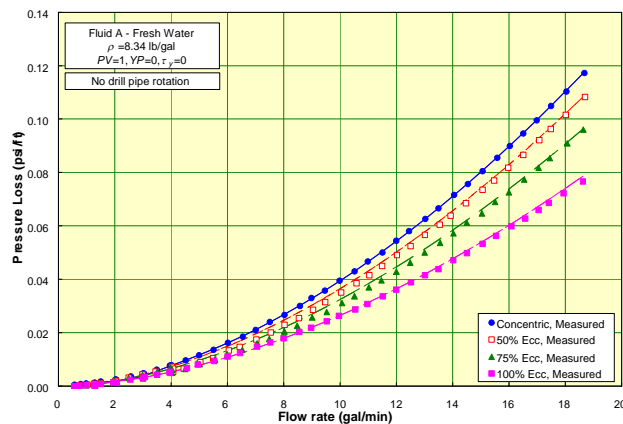| **Table 1** – Summary of fluids used for flow-loop testing							
Fluid ID	**Fluid Type**	**Figures**	**Density**	**PV**	**YP**	τ_y	**R**
			lb$_m$/gal	**cP**	**lb$_f$/100ft^2**	**lb$_f$/100ft^2**	τ_y/YP
A	Fresh water	1, 3	8.34	1	0	0	0
B	5% Cesium Formate	4	9.20	1	0	0	0
C	26-lb$_m$/bbl Bentonite slurry	5	8.72	35	37	14.7	0.40
D	Biopolymer field mud	2, 6	9.83	12	26	6.0	0.23
E	18-lb$_m$/bbl Bentonite slurry	7,8	8.53	4	1	0.5	0.50
F	0.5-lb$_m$/bbl Biopolymer	9,10	9.18	3	2	0.5	0.25
G	2-lb$_m$/bbl HEC	11-14	8.47	11	12	0	0

Fig. 1 - Effects of eccentricity on pressure loss with Fluid A without drill-pipe rotation. Markers show measured pressure losses; lines show calculated values.
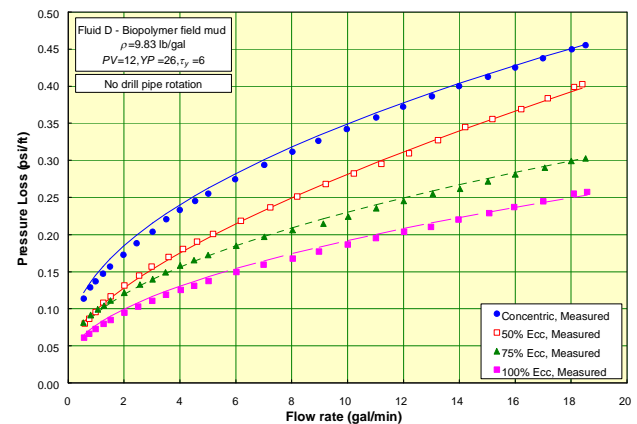

Fig. 2 - Effects of eccentricity on pressure loss with Fluid D without drill-pipe rotation. Markers show measured pressure losses; lines show calculated values.
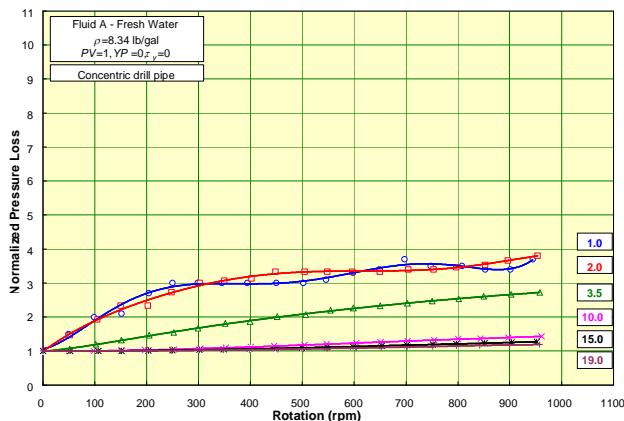
Fig. 3a - Effects of rotation on normalized pressure loss for Fluid A with concentric drill pipe. The number beside each curve indicates flow rate in gal/min.
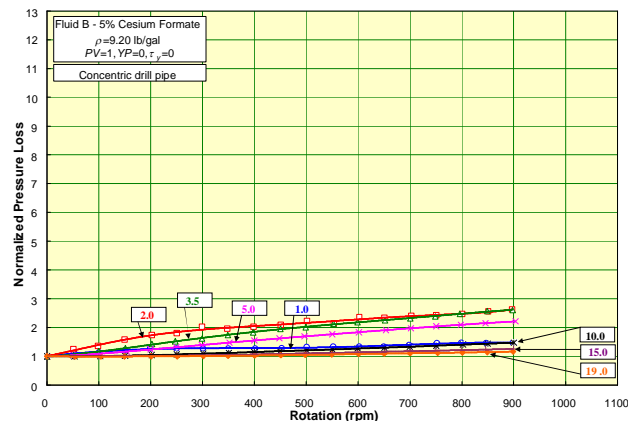

Fig. 4a - Effects of rotation on normalized pressure loss for Fluid B with concentric drill pipe. Numbers in the text boxes indicate flow rate in gal/min.
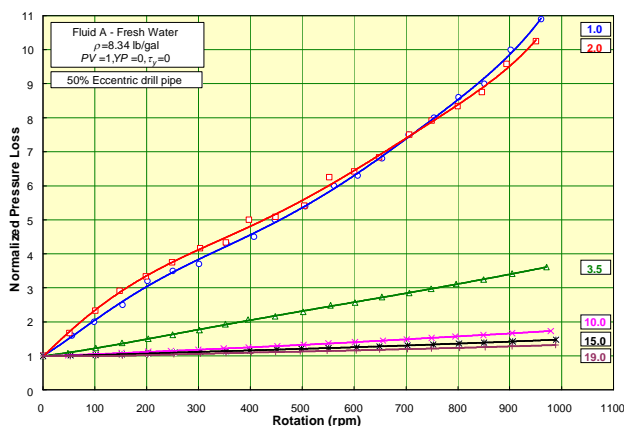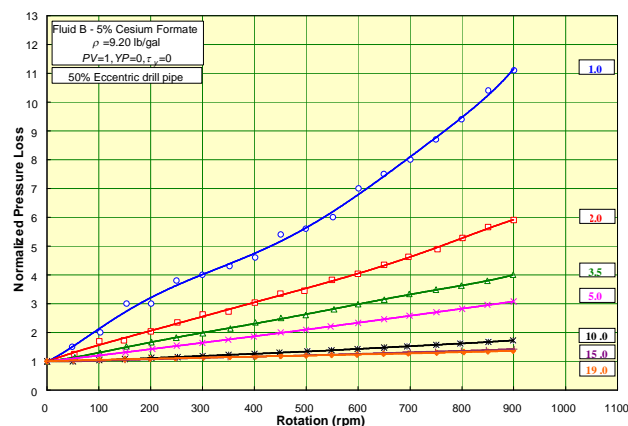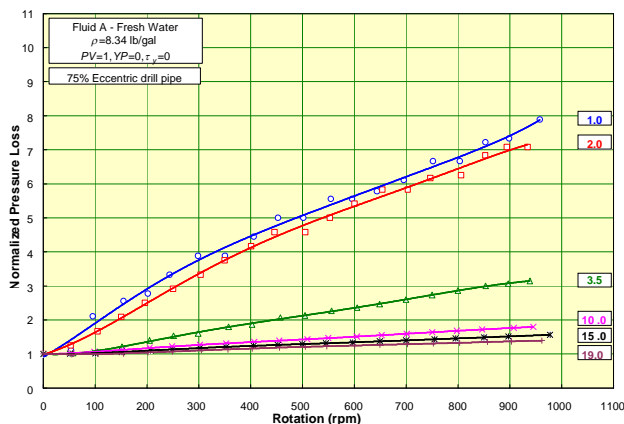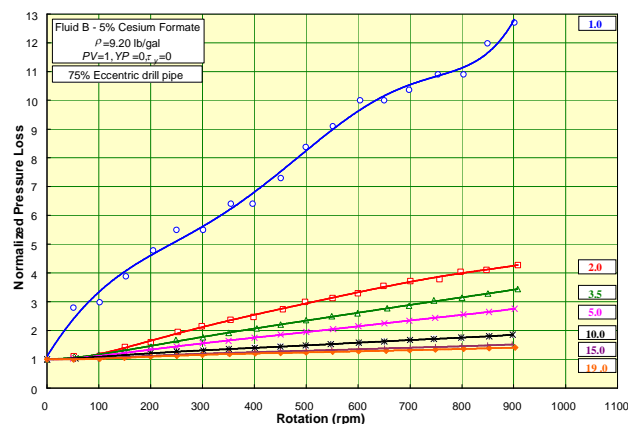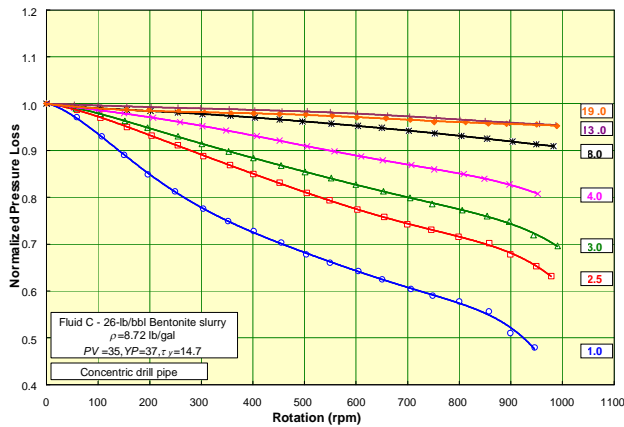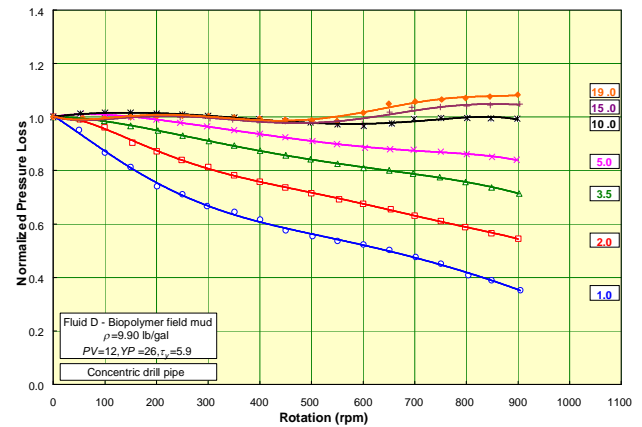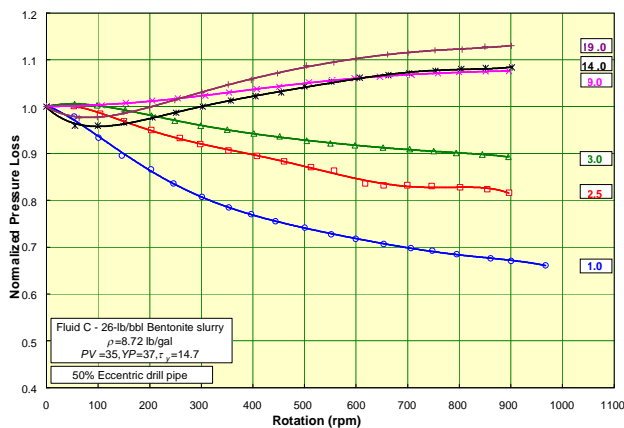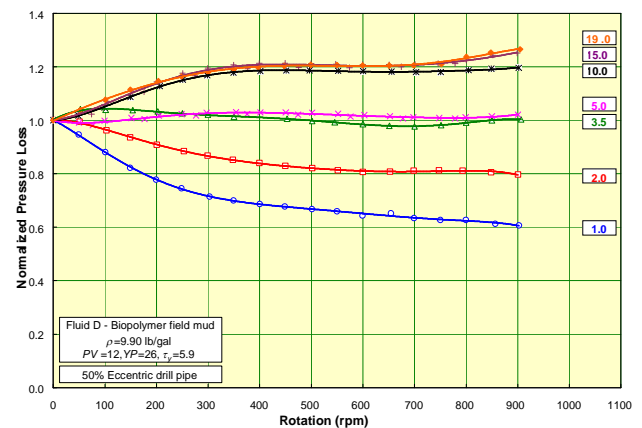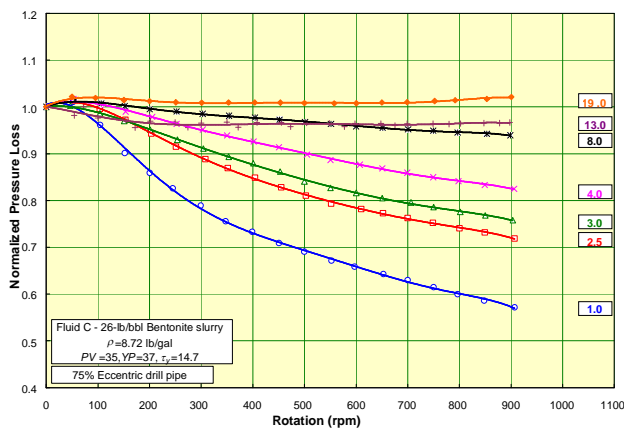

Fig. 3b - Effects of rotation on normalized pressure loss for Fluid A with 50% eccentric drill pipe. The number beside each curve indicates flow rate in gal/min.
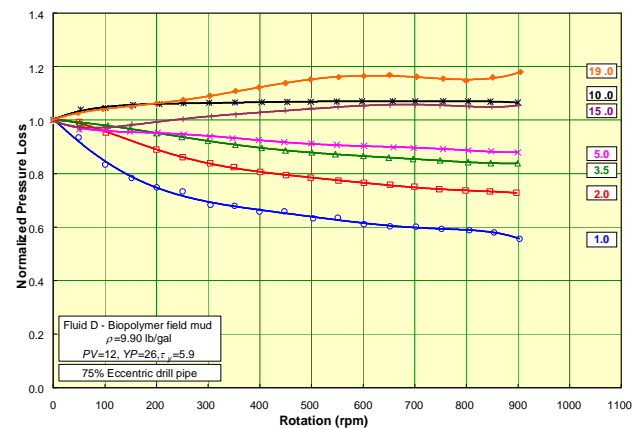

Fig. 4b - Effects of rotation on normalized pressure loss for Fluid B with 50% eccentric drill pipe. The number beside each curve indicates flow rate in gal/min.

Fig. 3c - Effects of rotation on normalized pressure loss for Fluid A with 75% eccentric drill pipe. The number beside each curve indicates flow rate in gal/min.
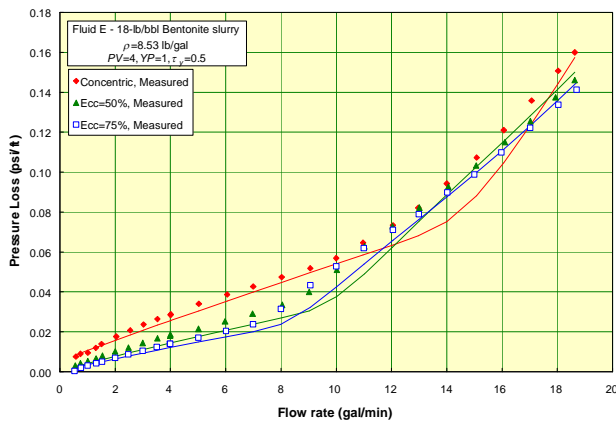

Fig. 4c - Effects of rotation on normalized pressure loss for Fluid B with 75% eccentric drill pipe. The number beside each curve indicates flow rate in gal/min.
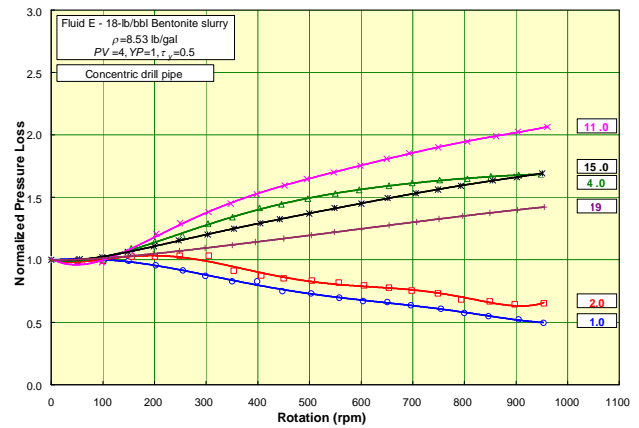
Fig. 5a - Effects of rotation on normalized pressure loss for Fluid C with concentric drill pipe. The number beside each curve indicates flow rate in gal/min.

Fig. 6a - Effects of rotation on normalized pressure loss for Fluid D with concentric drill pipe. The number beside each curve indicates flow rate in gal/min.
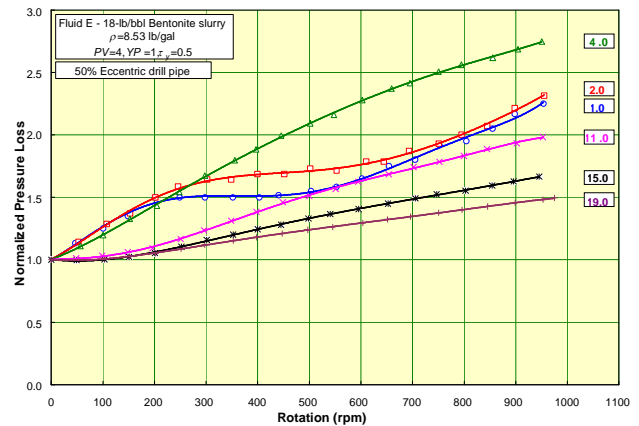

Fig. 5b - Effects of rotation on normalized pressure loss for Fluid C with 50% eccentric drill pipe. The number beside each curve indicates flow rate in gal/min.

Fig. 6b - Effects of rotation on normalized pressure loss for Fluid D with 50% eccentric drill pipe. The number beside each curve indicates flow rate in gal/min.
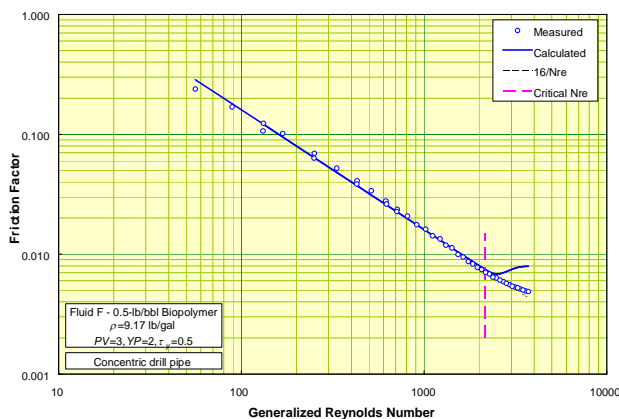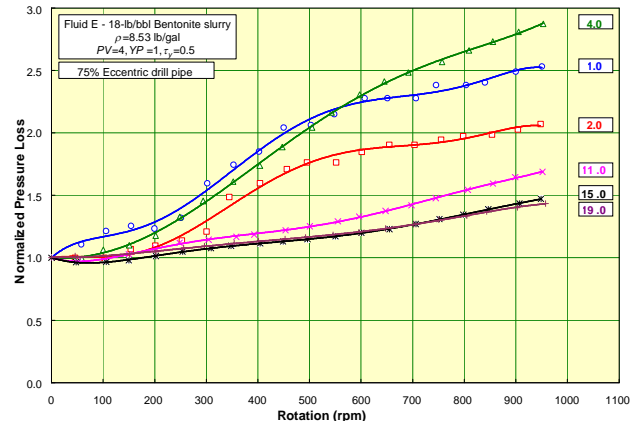

Fig. 5c - Effects of rotation on normalized pressure loss for Fluid C with 75% eccentric drill pipe. The number beside each curve indicates flow rate in gal/min.

Fig. 6c - Effects of rotation on normalized pressure loss for Fluid D with 75% eccentric drill pipe. The number beside each curve indicates flow rate in gal/min.
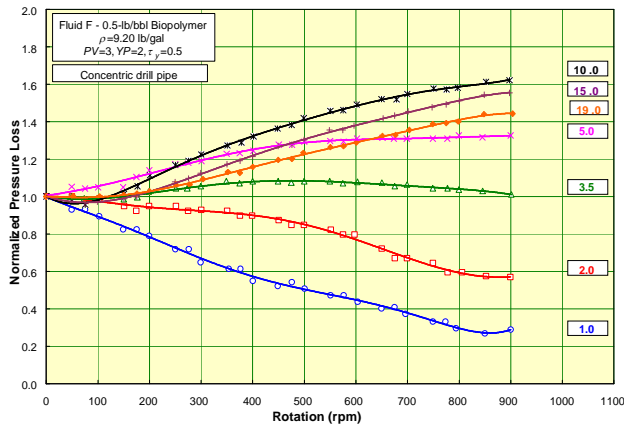
Fig. 7 – Effects of eccentricity on pressure loss with Fluid E without rotation. Markers show measured data, while lines indicate calculated values.

Fig. 8a - Effects of rotation on normalized pressure loss for Fluid E with concentric drill pipe. The number beside each curve indicates flow rate in gal/min.
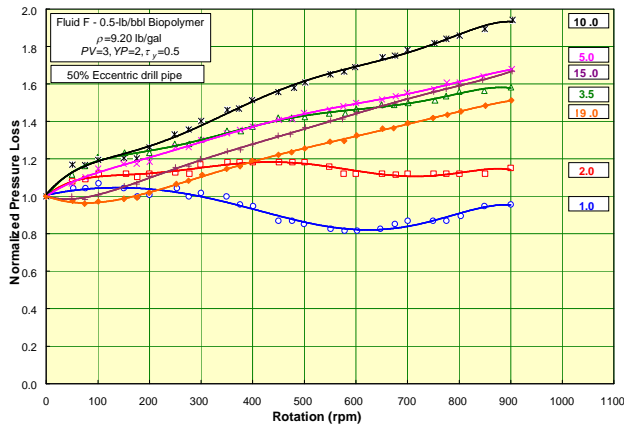

Fig. 8b - Effects of rotation on normalized pressure loss for Fluid E with 50% eccentric drill pipe. The number beside each curve indicates flow rate in gal/min.

Fig. 9 – Fluid F friction-factor plot showing drag reduction in turbulent flow.

Fig. 8c - Effects of rotation on normalized pressure loss for Fluid E with 75% eccentric drill pipe. The number beside each curve indicates flow rate in gal/min.
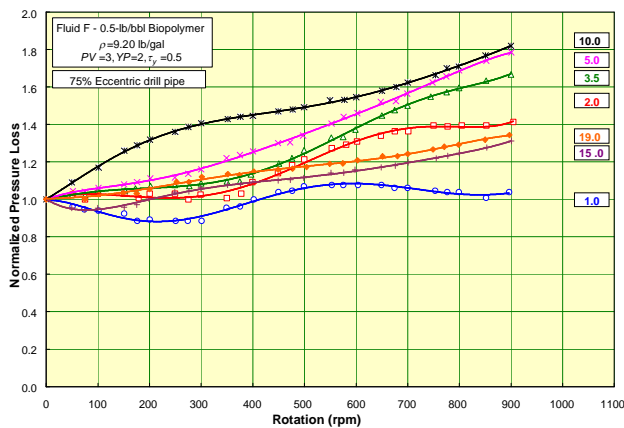
Fig. 10a - Effects of rotation on normalized pressure loss for Fluid F with concentric drill pipe. The number beside each curve indicates flow rate in gal/min.

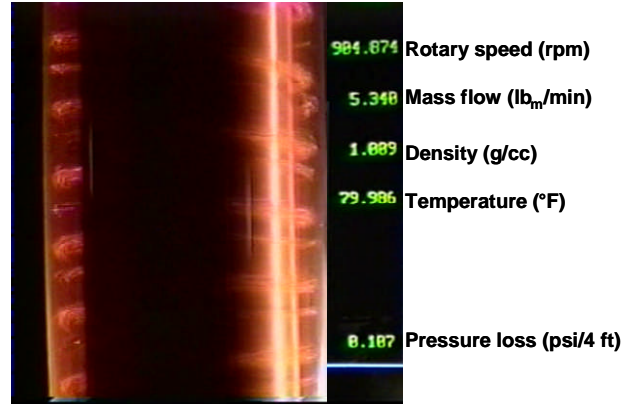**Fig. 11 –** Video image capture showing sensor data automatically superimposed over flow loop video.

Fig. 10b - Effects of rotation on normalized pressure loss for Fluid F with 50% eccentric drill pipe. The number beside each curve indicates flow rate in gal/min.

Fig. 10c - Effects of rotation on normalized pressure loss for Fluid F with 75% eccentric drill pipe. The number beside each curve indicates flow rate in gal/min.
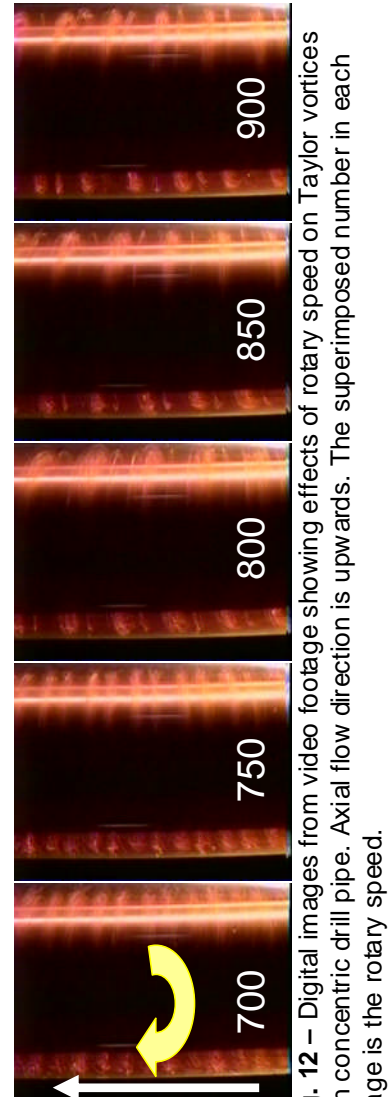

Fig. 12 – Digital images from video footage showing effects of rotary speed on Taylor vortices with concentric drill pipe. Axial flow direction is upwards. The superimposed number in each image is the rotary speed.
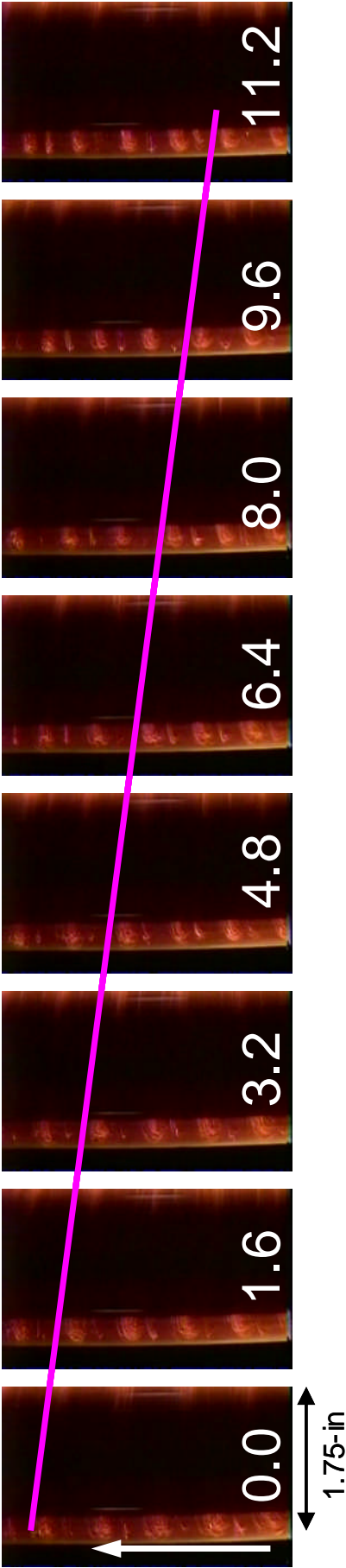
Fig. 13 – Digital images from video footage showing Taylor vortices at 900 rpm rotary speed. The superimposed number in each figure indicates elapsed time in seconds. Axial flow is upwards while Taylor vortices translate downwards opposite to the direction of flow. Solid line through images tracks position of an individual vortice. Wellbore diameter is 1.75 in.
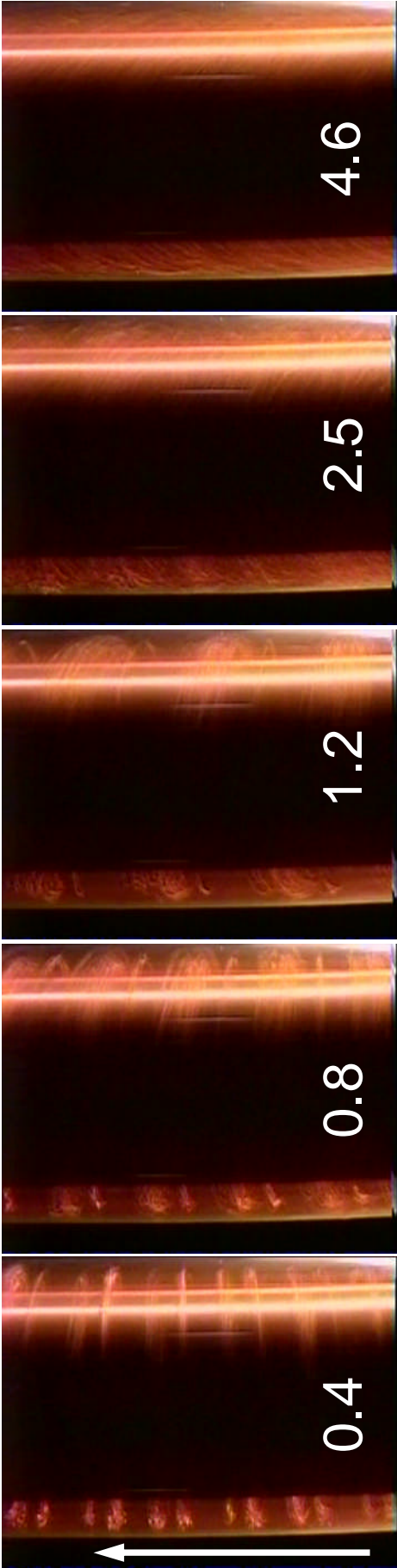

Fig. 14 – Digital images from video footage showing behavior of Taylor vortices with increasing axial flow. The superimposed number in each figure indicates axial flow rate in gal/min. Note Taylor vortices pattern change from toroidal to helical as axial flow rate is increased.